Resubmission of 8849R2

Ruizhongite, $(Ag_2\square)Pb_3Ge_2S_8$, a thiogermanate mineral from the Wusihe Pb–Zn deposit, Sichuan Province, Southwest China

YU-MIAO MENG[1], XIANGPING GU[2,*], SONGNING MENG[1,3], AND XIAO-WEN HUANG[1]

[1]State Key Laboratory of Ore Deposit Geochemistry, Institute of Geochemistry, Chinese Academy of Sciences, Guiyang 550081, China

[2]School of Geosciences and Info-Physics, Central South University, Changsha 410083, China

[3]College of Earth Sciences, Chengdu University of Technology, Chengdu 610059, China

*E-mail: guxp2004@163.com (XP Gu)

ABSTRACT

Ruizhongite (IMA2022-066), $(Ag_2\square)Pb_3Ge_2S_8$, is a thiogermanate of economic importance discovered in the Wusihe Pb–Zn deposit in Sichuan Province, southwestern China. This mineral occurs as anhedral grains 1–10 μm in size. It is gray and opaque, with a metallic luster and black streak, closely associated with galena and pyrite in a sphalerite matrix. Under reflected light microscope, it displays a greenish-gray color without internal reflection. Its reflectance values in air (R %) based on SiC as the reference material are 30.5, 32.2, 34, and 34.1 for corresponding wavelengths of 650, 589, 470, and 546 nm. According to the average of 18 electron microprobe analyses, Pb (57.37 wt%), S (21.39 wt%), Ge (11.53 wt%), Ag (7.34 wt%), Zn (1.57 wt%), and Fe (0.27 wt%) constitute 99.46 wt% of ruizhongite. The empirical formula based on the 8 S apfu is $(Ag_{0.82}Pb_{0.32}Zn_{0.28}Fe_{0.06})_{\Sigma 1.48}Pb_3Ge_{1.9}S_8$, and $(Ag_2\square)Pb_3Ge_2S_8$ is its ideal formula. Ruizhongite displays a cubic structure, space group $I\bar{4}3d$ (#220), with the unit-cell parameters a = 14.0559 (2), V = 2,777.00 (7), Z = 8, and the calculated density is 5.706 g/cm^3. The strongest powder X-ray diffraction lines [d in Å (I) (hkl)] are: 3.755 (100) (123), 3.511 (76) (004), 2.992 (73) (233), 2.574 (21) (125), 2.482 (79) (044), 2.276 (46) (235), 1.784 (39) (237), and 2.075 (24) (136). The structure of ruizhongite was determined using single-crystal XRD, and was refined to an R_1 of 0.0323 for all 2,594 (474 unique) reflections. The structure comprises a non-centrosymmetric arrangement of $[GeS_4]^{4-}$ tetrahedra, forming two interstice sites: fully-occupied Pb1 and partially-occupied Ag1, aligned in the directions of **a-**, **b-**, and **c-**axes. Ruizhongite was named in honor of Prof. Ruizhong Hu (1958), an eminent Chinese ore geochemist. The discovery of ruizhongite has significant implications for the occurrence and enrichment

47 mechanism of Ge in sphalerite and other metallic minerals.

48

49 **Keywords:** Ruizhongite, $(Ag_2□)Pb_3Ge_2S_8$, thiogermanate, Wusihe Pb–Zn deposit,

50 Sichuan, SW China

51

INTRODUCTION

Germanium (Ge) is an important element, which exhibits a low average crustal abundance of ~1.6 ppm (Taylor and McLennan 1985). Owing to its diverse applications including the production of fiber-optic systems, infrared optics, polyethylene catalysts, and solar cells, this element has been designated as a critical metal (USGS 2018). Considering that approximately 30% of Ge consumed around the world is produced from recycled materials, primary sources, such as zinc ore residues, coal ash, and flue dust, are unable to satisfy its demand (Frenzel et al. 2016; USGS 2018). China is a major producer of Ge, primarily as a byproduct of Pb–Zn ores, especially sphalerite and galena. The occurrence and enrichment mechanism of Ge have been investigated in many studies because of its economic importance.

According to Höll et al. (2007) and mindat.org, 37 naturally occurring Ge-bearing minerals have been identified and approved by the Commission of New Minerals, Nomenclature, and Classification of the International Mineralogical Association (IMA–CNMNC). Among them, 18 are Ge-sulfide minerals, with argyrodite, briartite, renierite, and germanite being relatively common. In laboratory, a series of thiogermanates, such as $(A_{1-2x}M_x)_2M_3Ge_2Q_8$ ($0 \leq x \leq 0.5$, A = Ag, Cu, Na; M = Pb, Eu, Ba; Q = S, Se), have been prepared, but their occurrence in nature has not been reported (Poduska et al. 2002; Iyer et al. 2004).

Ruizhongite, a thiogermanate mineral, was identified in the Wusihe Pb–Zn deposit in Sichuan Province, Southwest China, during an investigation of the mineralogy of this deposit. In the present study, the polarized optical microscopy, scanning electron microscopy, electron microprobe, μ-X-ray diffraction, and Raman spectroscopy analyses

were utilized to characterize the occurrence, optical property, chemical composition, and crystal structure of ruizhongite. Both the mineral and its name have been approved by the IMA–CNMNC (2022-066). Type specimens are preserved in the Geological Museum of China, Beijing, China (Catalog number M16138).

Ruizhongite was named in honor of Prof. Ruizhong Hu (1958) of the Institute of Geochemistry, Chinese Academy of Sciences (IGCAS). Prof. Hu obtained his Ph.D. from Chengdu College of Geology (currently known as Chengdu University of Technology) in 1988. Including 2 years of post-doctoral research, he has been working in the IGCAS since 1989, and earned a high reputation with over 200 publications and seven major awards on mineral resources and the geochemistry of ore deposits. These studies include the proposal of new methods and elucidation of intracontinental metallogenesis, and mechanisms of the formation of the ores involving critical metals such as Ge. In 2021, he was elected a member of the Chinese Academy of Sciences. In the present study, the morphology, composition, physical properties, and crystallography of ruizhongite are described. A comparison with synthetic analogs including $AgPb_{0.5}Pb_3Ge_2S_8$, $PbPb_3Ge_2S_8$, and $(CuPb_{0.5})Pb_3Ge_2S_8$ is also provided.

OCCURRENCE AND ORIGIN

Ruizhongite occurs in the Wusihe Pb–Zn deposit at E102°53'23.0″ and N29°16'27.0″, approximately 25 km southeast of the Hanyuan County, Sichuan Province. This deposit is estimated to contain 3.7 Mt of Pb and Zn with grades of 8.6 and 2.0%, respectively (Xiong et al. 2018). The Wusihe deposit is part of the Sichuan–Yunnan–Guizhou (SYG) Pb–Zn metallogenic province in the western Yangtze Block (Online

Appendix Materials Fig. OM1a; Wang 2005; Zheng 2012). Exposed rocks in the Wusihe deposit area comprise mainly of the Ediacaran Dengying Formation and Cambrian to Permian marine sequences (Online Appendix Materials Fig. OM1b). Mineralization in the Wusihe deposit was controlled primarily by the Wangmaoshan and Maotuo faults, and ore bodies are hosted predominantly in carbonaceous shales of the Lower Cambrian Qiongzusi Formation and siliceous dolomites of the Dengying Formation (Online Appendix Materials Fig. OM1b). The contact zone between the Qiongzusi and Dengying formations also hosts some ore bodies. Regardless that the ores are either massive, disseminated, or vein-type, the mineral assemblages are similar.

The Wusihe deposit has been characterized as an MVT that formed at ~411 Ma (Xiong et al. 2018), and according to previous studies, the Pb and Zn originated from both the basement and host rocks (e.g., Xiong et al. 2018; Zhang et al. 2019; Wei et al. 2020). Sphalerite samples that were collected from the deposit have Ge concentrations that range from ~3 to 1,934 ppm (mean = 563 ppm), attributed to substitution of Zn (Luo et al. 2021). Ruizhongite occurs as tiny disseminated grains, 1 to 10 μm in size, in close association with galena, jordanite, and argutite in the sphalerite matrix (Fig. 1).

EXPERIMENTAL METHODS AND RESULTS

Physical and optical properties

Ruizhongite is gray with a black streak and the Mohs hardness is estimated to be 3 to 3.5 (comparable to that of jordanite). It is brittle without cleavage. The calculated density is 5.706 g/cm^3 based on the empirical formula and unit cell volume refined from single-crystal XRD data. According to tests using a magnetic needle, the mineral is

nonmagnetic.

In reflected light, ruizhongite shows a greenish gray color (Fig. 1a–d) without bireflectance, pleochroism, anisotropy, or internal reflection. Reflectance values measured in air by Leitz MSP-UV-VIS 2000 microphotospectrometer using SiC as the reference material are presented in Table 1.

Raman spectroscopy

Raman spectra for ruizhongite were obtained using a Horiba ARAMIS micro-Raman system at the School of Geosciences and Info-physics, Central South University. A solid-state laser instrument with a wavelength of 532 nm and a thermoelectric-cooled CCD detector with a resolution of 2 cm^{-1} and a spot size of 1 μm was used for excitation. Raman spectra were acquired from 100 to 1,000 cm^{-1}, and the measurement time for each spectrum was 180 s. Polished thin sections of randomly oriented ruizhongite crystals were utilized for the Raman spectroscopy measurements. In a typical spectrum, sharp peaks are observed at 81, 217, and 348 cm^{-1}, whereas intermediate peaks are visible at 111 and 406 cm^{-1}, and weak peaks are present at 261 and 361 cm^{-1} (Fig. 2a). The Raman spectrum of ruizhongite is comparable to that of synthetic $Ag_{0.5}Pb_{1.75}GeS_4$ (Fig. 2b, Iyer et al. 2004). The peaks between 300 and 500 cm^{-1} can be assigned to Ge–S stretching vibrations in GeS_4 tetrahedra, whereas peaks lower than 300 cm^{-1} are attributed to S–Ge–S bending vibrations in GeS_4 tetrahedra, as well as Pb–S and (Ag, Pb, Zn)–S stretching vibrations.

Chemical composition

144 The chemical composition of ruizhongite was characterized using a Shimadzu-1720
145 electron microprobe via the wavelength dispersive spectrometry. Measurements were
146 conducted at the School of Geosciences and Info-physics, Central South University, and
147 the acceleration voltage, beam current, and beam size were 15 kV, 10 nA, and 1 μm,
148 respectively. A qualitative scan of elements reveals the presence of S, Pb, Fe, Ag, Zn, and
149 Ge, and the quantitative analyses were made using pure Ge, PbS, Ag, ZnS, and FeS_2 as
150 standards, and the ZAF4 program of the instrument was used for correction. Data for the
151 composition of ruizhongite are presented in Table 2. Average data from the 18 analyses
152 yield Pb (57.37 wt%), S (21.39 wt%), Ge (11.53 wt%), Ag (7.34 wt%), Zn (1.57 wt%),
153 and Fe (0.27 wt%), with a total of 99.46 wt%. The empirical formula calculated on the
154 basis of 8 S apfu was $(Ag_{0.82}Pb_{0.32}Zn_{0.28}Fe_{0.06})_{\Sigma 1.48}Pb_3Ge_{1.90}S_8$, and the simplified formula
155 is (Ag, Pb, Zn, Fe, □)$_3$$Pb_3Ge_2S_8$. According to the crystal structure and IMA rule of
156 endmember (Hatert and Burke, 2008), the ideal formula is $(Ag_2□)Pb_3Ge_2S_8$.
157

158 ## Crystallography and crystal structure

159 A single crystal of ruizhongite about 6*5*4 μm^3 (Fig. 1d) was extracted for X-ray
160 diffraction by focused ion (Ga+) beam (FIB) workstation equipped in the FEI Helios
161 Nanolab 600i systems at the National Key Lab of Powder Metallurgy, Central South
162 University. Powder XRD measurements were performed using a Rigaku XtaLAB
163 Synergy diffractometer. Measurements were conducted using Cu*K*α radiation at 50 kV
164 and 1 mA in the Gandolphi powder mode. However, only incomplete lines are observed
165 due to the extremely small size of sample. Thus, calculated X-ray powder diffraction data
166 according to the crystal structure are presented (Table 3). The strongest lines [*d* in Å (*I*)

(*hkl*)] are: 3.755 (100) (123), 3.511 (76) (004), 2.992 (73) (233), 2.574 (21) (125), 2.482 (79) (044), 2.276 (46) (235), 1.784 (39) (237), and 2.075 (24) (136). The refined unit cell parameters from powder X-ray diffraction data are: a = 14.0443 (5) Å, V = 2770.14 (28) Å^3, and Z = 8.

Single-crystal XRD measurements were conducted using a Rigaku XtaLAB Synergy-DS diffractometer at the School of Geosciences and Info-physics, Central South University, China. The instrument, which involves a microfocus-sealed Cu anode tube, was operated at 50 kV and 1mA. The unit-cell parameters are: a = 14.0559 (2) Å, V = 2,777.00 (7) Å^3, and Z = 8. Based on reflection data, the candidate space group is $I\bar{4}3d$ (#220). The Rigaku *CrysAlisPro* software package was used to process diffraction data including the Lorentz and polarization corrections. An empirical absorption correction was employed via a multi-scan method using ABSCOR (Higashi 2001).

The crystal structure of ruizhongite was determined and refined using the SHELX (Sheldrick 2015a, b) and Olex2 (Dolomanov et al. 2009) packages. Crystallographic and refinement statistics data are presented in Table 4. The structure based on the $I\bar{4}3d$ space group involves two anion (S1 and S2) and three cation (Ge1, Pb1, and Ag1) sites (Fig. 3a). According to a refinement, the Ge1 and Pb1 sites are fully occupied, whereas Ag1 is partially occupied. Therefore, based on compositional data, the occupancies of Ag, Pb, Zn, and Fe at Ag1 site were manually adjusted. The atomic coordinates and displacement parameters are presented in Table 5, while selected bond lengths and angles are listed in Table 6. The final anisotropic full-matrix least-squares refinement of F^2 was converged to an R_1 of 2.98% and wR_2 of 6.66% for the 447 independent reflections (F0> 4σ) and an R_1 of 3.23% and wR_2 of 6.76% for all 2,594 (474 unique) reflections (Table 4).

Ruizhongite is isostructural with synthetic $Ag_{0.5}Pb_{1.75}GeS_4$ (Iyer et al. 2004) and Pb_2GeS_4 (Poduska et al. 2002). The structure involves a non-centrosymmetric arrangement of $[GeS_4]^{4-}$ tetrahedra, with interstices occupied by Pb1 and Ag1 aligned along the ***a***-, ***b***-, and ***c***-axes (Fig. 3b). The Ge-S bond lengths in the slightly distorted $[GeS_4]^{4-}$ tetrahedra vary from 2.208 to 2.242 Å (mean = 2.217 Å) (Table 6). The Pb1 is coordinated to four sulfur atoms, forming pyramid-like geometry at distances ranging from 2.839 to 2.868 Å (mean = 2.854 Å) (Fig. 3a and c), and to four additional sulfur atoms at distances that vary from 3.421 to 3.468 Å. In contrast, the Ag1 site is partially occupied by Ag (0.28), Pb (0.12), Zn (0.10), and Fe (0.02), and coordinated to four sulfur atoms thereby in a shape of quadrangles at distances from 2.708 to 2.898 Å (Fig. 3a and c). The Ag1 sites are clustered and aligned along the ***a***-, ***b***-, and ***c***-axes, and the Ag1–Ag1 distance is 0.717 Å (Table 6 and Fig. 3b).

DISCUSSION

Ruizhongite is the first natural occurrence of non-centrosymmetric cubic thio- and seleno-germanates with the following general formula: $(A_{1-2x}M_x)_2M_3Ge_2Q_8$ ($0 \leq x \leq 0.5$, A = Ag, Cu, Na; M = Pb, Eu, Ba; Q = S, Se), that have been produced in the laboratory (e.g., Poduska et al. 2002; Iyer et al. 2004; Choudhury et al. 2007; Reshak et al. 2013). This group can be extended to include thiostannates with similar cubic structure and space group, such as $Ag_2CdBa_6Sn_4S_{16}$ and $Ba_3CdSn_2S_8$, if A = Ag, Cd, M = Ba, and Q = Sn (e.g., Teske 1985; Zhen et al. 2016). The $Ba_3CdSn_2S_8$ has strong tolerance ability for vacancies and disorder, and thus many elements can be substituted into its structure (Iyer et al. 2004). Moreover, the $Ba_3CdSn_2S_8$ structure can be formed with different tetrahedral units

such as $[PSe_4]^{3-}$, $[GeS_4]^{4-}$, or $[SnS_4]^{4-}$ when cation sites were substituted by +1 or +2 metals with or without introducing disorder and/or vacancies (Aitken et al. 2000). This makes it becomes a good candidate for tuning of properties. Therefore, it can be predicted that more minerals with similar structure can be present in nature or synthetized in laboratory. Iyer et al. (2004) inferred that a series of compounds such as $Sr_{0.5}Pb_{1.5}GeQ_4$, $Sr_{0.25}Pb_{1.75}GeQ_4$, $Na_{0.5}Sn_{1.75}GeQ_4$, $Cu_{0.5}Eu_{1.75}SnQ_4$, and $Cu_{1.5}Pb_{0.75}AsQ_4$ (Q = S, Se) can be present. Therefore, Sr- or Na-bearing Ge minerals will be the important target of new minerals in the future. Considering that Na and Sr are incompatible in sulfides such as sphalerite, galena and pyrite, the discovery of Sr- or Na-bearing Ge minerals should focus on gangue minerals such as calcite, dolomite, and feldspar.

Crystallographic data for ruizhongite, synthetic $(AgPb_{0.5})Pb_3Ge_2S_8$, $PbPb_3Ge_2S_8$, and $(CuPb_{0.5})Pb_3Ge_2S_8$ are presented in Table 7. The ruizhongite and synthetic $Ag_{0.5}Pb_{1.5}GeS_4$ have the same Ge-S distance but slightly different M-S and A-S distances. These differences indicate that significant variations in bond lengths at *A* and *M* sites may be caused with the replacement of Ag by Cu and more incorporation of Pb into *A* sites, whereas GeS_4 tetrahedra are just slightly altered. Compared to synthetic $Ag_{0.5}Pb_{1.5}GeS_4$, the Raman spectra of ruizhongite shows characteristic peaks at 81 cm^{-1} and 111 cm^{-1} (Fig. 2a). This difference in Raman spectra is possibly caused by minor amounts of Zn and Fe in ruizhongite.

The synthetic compounds are mainly produced by high temperature (510-650°C) heating and annealing processes (Poduska et al. 2002; Iyer et al. 2004), which may provide constraints on the formation condition of ruizhongite from the Wusihe deposit. The pure crystal of $Ag_{0.5}Pb_{1.75}GeS_4$ can be obtained by direct combination of the

elements at 650°C in a sealed silica tube set in a furnace, cooling to 250°C at the rate of 5 °C/h and then rapidly cooling to room temperature (Iyer et al. 2004). It is thus inferred that ruizhongite may have been formed at a rapid cooling rate from initial Ge-bearing fluids.

Ruizhongite appears chemically related to morozeviczite ($Pb_3Ge_{1-x}S_4$) (Harańczyk 1975; Anthony et al. 2016). However, the significant differences in the unit cell parameters (a = 10.61 Å) and powder XRD data (3.08 (10), 2.15 (9), 2.80 (6), 2.047 (6), and 1.791 (5)) exclude the possibility of morozeviczite being Pb-dominated at the disordered Ag1 site in ruizhongite.

IMPLICATIONS

Thiogermanate minerals are the principal carriers of Ge in nature. There are 17 thiogermanate minerals identified according to the data of www.mindat.org. Ruizhongite is the Ag endmember with the Ag1 site dominated by Ag in a group of non-centrosymmetric cubic thio- and seleno-germanate isostructural analogues, and the variation of chemical composition also indicate possible endmembers of $(Pb\square_2)Pb_3Ge_2S_8$, $(Zn\square_2)Pb_3Ge_2S_8$, and $(Fe\square_2)Pb_3Ge_2S_8$.

Sphalerite may be an important bearer of Ge, because the ionic radii of Ge^{2+} is similar to Zn^{2+} (0.73–0.74 Å), but significantly different from Ge^{4+} (0.39–0.53 Å) (Shannon, 1976). In previous studies, mechanisms for the substitution of Zn with Ge, including the simple and coupled substitution, have been proposed (e.g., Höll et al. 2007; Cook et al. 2009; Belissont et al. 2014). The discovery of ruizhongite in sphalerite further supports the existence of nanometric to micrometric Ge independent minerals in

sphalerite under a local and relatively oxidized environment, in addition to those associated with isomorphic substitution. Therefore, correlations between the concentrations of Ge and those of Ag, Pb, and Fe for sphalerite samples that are determined using laser ablation ICP-MS must be treated with caution in regard to Ge substitution mechanisms in sphalerite. High-resolution scanning and transmission electron microscopy were also needed to characterize Ge-containing minerals in the sphalerite or some other samples.

The presence of ruizhongite in sphalerite indicates that fluids responsible for sphalerite were periodically supersaturated with Ge. However, based on available data, the formation mechanism of ruizhongite remains obscure. Therefore, Ge-rich fluids and physicochemical conditions associated with the formation of ruizhongite in sphalerite require further investigation. The composition of ruizhongite suggests a close relationship between Ge and Pb, and thus, factors controlling the affinity of Ge for Pb relative to Zn also require attention. Therefore, improved understanding of geochemical characteristics during the crystallization of sphalerite and galena can highlight the mechanism of Ge enrichment in Pb–Zn deposits.

ACKNOWLEDGMENTS

We thank Shaohua Dong for her assistance with the SEM analysis, as well as Ming Wang at the Wusihe deposit of Sichuan Qiansheng Mining Co., Ltd., and Chuan Lv and Yunhe Zhou of the IGCAS for their help with the field investigation. This research was financially supported by the National Key Research and Development Program of China (Grant No. 2021YFC2900300), National Natural Science Foundation of China

(42073043, 42072054), CAS Hundred Talents Program to XWH, Field Frontier Key Project of State Key Laboratory of the Ore Deposit Geochemistry (202101), and Guizhou Provincial 2020 Science and Technology Subsidies (No. GZ2020SIG). The manuscript was improved based on critical comments of Prof. Luca Bindi and two anonymous reviewers.

REFERENCES CITED

Aitken, J.A., Marking, G.A., Evain, M., Iordanidis, L., and Kanatzidis, M.G. (2000) Flux synthesis and isostructural relationship of cubic $Na_{1.5}Pb_{0.75}PSe_4$, $Na_{0.5}Pb_{1.75}GeS_4$, and $Li_{0.5}Pb_{1.75}GeS_4$. Journal of Solid State Chemistry, 153(1), 158-169.

Anthony, J.W., Bideaux, R.A., Bladh, K.W., and Nichols, M.C. (2016) Handbook of Mineralogy. Mineralogical Society of America, Chantilly, USA.

Belissont, R., Boiron, M.-C., Luais, B., and Cathelineau, M. (2014) LA-ICP-MS analyses of minor and trace elements and bulk Ge isotopes in zoned Ge-rich sphalerites from the Noailhac–Saint-Salvy deposit (France): Insights into incorporation mechanisms and ore deposition processes. Geochimica et Cosmochimica Acta, 126, 518-540.

Brese, N., and O'keeffe, M. (1991) Bond-valence parameters for solids. Acta Crystallographica Section B: Structural Science, 47(2), 192-197.

Choudhury, A., Polyakova, L.A., Strobel, S., and Dorhout, P.K. (2007) Two non-centrosymmetric cubic seleno-germanates related to CsCl-type structure: Synthesis, structure, magnetic and optical properties. Journal of Solid State Chemistry, 180(4), 1381-1389.

Cook, N.J., Ciobanu, C.L., Pring, A., Skinner, W., Shimizu, M., Danyushevsky, L.,

Saini-Eidukat, B., and Melcher, F. (2009) Trace and minor elements in sphalerite: A LA-ICPMS study. Geochimica et Cosmochimica Acta, 73(16), 4761-4791.

Dolomanov, O.V., Bourhis, L.J., Gildea, R.J., Howard, J.A.K., and Puschmann, H. (2009) A complete structure solution, refinement and analysis program. Journal of Applied Crystallography, 42(2), 339-341.

Frenzel, M., Hirsch, T., and Gutzmer, J. (2016) Gallium, germanium, indium, and other trace and minor elements in sphalerite as a function of deposit type—A meta-analysis. Ore Geology Reviews, 76, 52-78.

Haranczyk, C. (1975) Morozeviczite and polkovicite, typochemical minerals of Mesozoic mineralization of the Fore-Sudenten monocline. Rudy Metalle, 20(2), 288-293.

Hatert, F. and Burke, E. A. J. (2008) The IMA-CNMNC dominant-constituent rule revisited andextended. Canadian Mineralogist, 46, 717-728.

Higashi, T. (2001) ABSCOR, Tokyo. Rigaku Corporation.

Höll, R., Kling, M., and Schroll, E. (2007) Metallogenesis of germanium-A review. Ore Geology Reviews, 30(3-4), 145-180.

Hu, R., Fu, S., Huang, Y., Zhou, M.-F., Fu, S., Zhao, C., Wang, Y., Bi, X., and Xiao, J. (2017) The giant South China Mesozoic low-temperature metallogenic domain: Reviews and a new geodynamic model. Journal of Asian Earth Sciences, 137, 9-34.

Iyer, R.G., Aitken, J.A., and Kanatzidis, M.G. (2004) Noncentrosymmetric cubic thio-and selenogermanates: $A_{0.5}M_{1.75}GeQ_4$ (A=Ag, Cu, Na; M=Pb, Eu; Q=S, Se). Solid State Sciences, 6(5), 451-459.

Luo, K., Zhou, J., Xu, Y., He, K., Wang, Y., and Sun, G. (2021) The characteristics of the extraordinary germanium enrichment in the Wusihe large-scale Ge-Pb-Zn deposit,

328 Sichuan Province, China and its geological significance. Acta Petrologica Sinica,
329 37(9), 2761-2777 (in Chinese with English abstract).
330 Poduska, K.M., Cario, L., DiSalvo, F.J., Min, K., and Halasyamani, P.S. (2002) Structural
331 studies of a cubic, high-temperature (α) polymorph of Pb_2GeS_4 and the isostructural
332 $Pb_{2-x}Sn_xGeS_{4-y}Se_y$ solid solution. Journal of Alloys Compounds, 335(1-2), 105-110.
333 Reshak, A.H., Kogut, Y.M., Fedorchuk, A.O., Zamuruyeva, O.V., Myronchuk, G.L.,
334 Parasyuk, O.V., Kamarudin, H., Auluck, S., Plucinski, K.J., and Bila, J. (2013)
335 Electronic and optical features of the mixed crystals $Ag_{0.5}Pb_{1.75}Ge(S_{1-x}Se_x)_4$. Journal
336 of Materials Chemistry 1(31), 4667-4675.
337 Shannon, R.D. (1976) Revised Effective Ionic Radii and Systematic Studies of
338 Interatomic Distances in Halides and Chalcogenides. Acta Crystallographica, A32,
339 751-767.
340 Sheldrick, G.M. (2015a) Crystal structure refinement with SHELXL. Acta
341 Crystallographica Section C: Structural Chemistry, 71(1), 3-8.
342 Sheldrick, G.M.A. (2015b) SHELXT–Integrated space-group and crystal-structure
343 determination. Acta Crystallographica Section A: Foundations Advances, 71(1), 3-8.
344 Taylor, S.R., and McLennan, S.M. (1985) The continental crust: its composition and
345 evolution. Blackwell Scientific Publisher, Palo Alto, CA. p.312.
346 Teske, C.L. (1985) Darstellung und Kristallstruktur von $Ba_3CdSn_2S_8$ mit einer
347 Anmerkung über $Ba_6CdAg_2Sn_4S_{16}$. Zeitschrift fuer Anorganische und Allgemeine
348 Chemie, 522(3), 122-130.
349 USGS. (2018) Germanium Statistics and Information. National Minerals Information
350 Center, United States Geological Survey, Virgina, USA,

https://www.usgs.gov/centers/national-minerals-information-center/germanium-statistics-and-information.

Wang, W. (2005) Texture and Structure Characteristics of Ore and Genetic Research of Wusihe Pb-Zn Deposit, Sichuan Province, Master, p. 109. China University of Geosciences (Wuhan), Wuhan.

Wei, C., Ye, L., Li, Z., Hu, Y., Huang, Z., Liu, Y., and Wang, H. (2020) Metal sources and ore genesis of the Wusihe Pb-Zn deposit in Sichuan, China: New evidence from in-situ S and Pb isotopes. Acta Petrologica Sinica, 36(12), 3783-3796 (in Chinese with English abstract).

Xiong, S.-F., Gong, Y.-J., Jiang, S.-Y., Zhang, X.-J., Li, Q., and Zeng, G.-P. (2018) Ore genesis of the Wusihe carbonate-hosted Zn-Pb deposit in the Dadu River Valley district, Yangtze Block, SW China: evidence from ore geology, S-Pb isotopes, and sphalerite Rb-Sr dating. Mineralium Deposita, 53(7), 967-979.

Zhang, H., Fan, H., Xiao, C., Wen, H., Ye, L., Huang, Z., Zhou, J., and Guo, Q. (2019) The mixing of multi-source fluids in the Wusihe Zn–Pb ore deposit in Sichuan Province, Southwestern China. Acta Geochimica, 38(5), 642-653.

Zhen, N., Wu, K., Wang, Y., Li, Q., Gao, W., Hou, D., Yang, Z., Jiang, H., Dong, Y., and Pan, S. (2016) $BaCdSnS_4$ and $Ba_3CdSn_2S_8$: syntheses, structures, and non-linear optical and photoluminescence properties. Dalton Transactions, 45(26), 10681-10688.

Zheng, X. (2012) Geological features and genesis of WuSiHe Pb-Zn deposit, Sichuan, Master thesis, p. 75. Chang'an University, Xi'an (in Chinese with English abstract).

Figure captions

Figure 1. Reflected light photomicrographs (**a**, **b**, **c**, **d**) and back scattered electron images (**e**, **f**) showing the occurrence of ruizhongite and associated minerals including: (**a**) Subhedral and anhedral grains of ruizhongite and pyrite disseminated in sphalerite. (**b**) Ruizhongite in sphalerite exhibiting an exsolution texture and euhedral or subhedral pyrite grains disseminated in sphalerite. (**c**) Ruizhongite at the contact between sphalerite and galena grains and jordanite inclusions in galena. (**d**) Ruizhongite and argutite as inclusions in sphalerite, and the grain was extracted by FIB to investigate the crystal structure. (**e**) An enlarged view of an area similar to that in (c). Under the BSE imaging, the gray color of ruizhongite is similar to that of jordanite. (**f**) An enlarged view of the area in (d). * Abbreviations: Agt, argutite; Rzh, ruizhongite; Py, pyrite; Sp, sphalerite; Gn, galena; Jrd, jordanite

Figure 2. Raman spectrum of ruizhongite compared to that of synthetic $Ag_{0.5}Pb_{1.75}GeS_4$ (Iyer et al. 2004). Considering that no peak is present after 500 cm^{-1}, the portion of the spectrum from 500 to 1,500 cm^{-1} is not shown.

Figure 3. Crystal structure of ruizhongite obtained using the Olex2 (Dolomanov et al. 2009) and VESTA (Momma and Izumi 2011) packages showing: (**a**) Sites of atoms and connectivity with highlighted the GeS_4 tetrahedron. (**b**) Structure projected on the (100) plane, displaying the distribution of GeS_4 tetrahedron, the alignment of Pb1, and clustered Ag1. (**c**) Distribution of GeS_4 tetrahedron and bonding geometry of Pb1-S and Ag1-S in the unit cell.

TABLE 1. Reflectance data for ruizhongite

R	λ (nm)	R	λ (nm)
28.2	400	33.5	560
28.3	420	32.6	580
31.3	440	32.2	589 (COM)
33.3	460	31.7	600
34.0	470 (COM)	31.0	620
34.5	480	30.6	640
34.9	500	30.5	650 (COM)
34.8	520	30.6	660
34.3	540	31.2	680
34.1	546 (COM)	32.5	700

This is the peer-reviewed, final accepted version for American Mineralogist, published by the Mineralogical Society of America.
The published version is subject to change. Cite as Authors (Year) Title. American Mineralogist, in press.
DOI: https://doi.org/10.2138/am-2023-9000. http://www.minsocam.org/

TABLE 2. Chemical composition of ruizhongite (in wt%)

Point	S	Pb	Fe	Ag	Zn	Ge	Total
Reference Material	Pure FeS_2	Pure PbS	Pure FeS_2	Pure Ag	Pure ZnS	Pure Ge	
$AgPb_{0.5}Pb_3Ge_2S_8$	20.77	58.73	0	8.74		11.76	100.00
rz-w01	21.24	57.90	0.20	7.90	1.54	11.69	100.47
rz-w02	21.59	56.41	0.08	7.64	1.62	11.48	98.82
rz-w03	21.51	57.83	0.09	7.65	1.64	11.84	100.55
rz-w04	21.57	58.31	0.29	6.60	1.54	11.47	99.78
rz-w05	21.44	58.17	0.32	6.42	1.61	11.65	99.62
rz-w06	21.76	57.21	0.99	6.68	1.58	11.42	99.63
rz-w07	21.41	56.70	0.38	7.28	1.65	11.40	98.81
rz-w08	21.48	58.15	0.02	7.56	1.37	11.76	100.34
rz-w09	21.29	57.61	0.00	7.40	1.46	11.72	99.48
rz-w10	21.52	58.00	0.00	7.62	1.47	11.47	100.07
rz-w11	21.61	58.09	0.07	7.35	1.39	11.35	99.85
rz-w12	20.76	56.41	0.23	7.14	1.57	11.75	97.84
rz-w13	21.04	57.30	0.27	7.41	1.62	11.37	99.01
rz-w14	21.22	57.07	0.29	7.58	1.72	11.50	99.38
rz-w15	21.48	56.69	0.28	7.43	1.71	11.31	98.91
rz-w16	21.40	57.23	0.32	7.53	1.63	11.54	99.65
rz-w17	21.49	56.37	0.53	7.47	1.46	11.53	98.84
rz-w18	21.25	57.20	0.47	7.43	1.62	11.28	99.23
Average	21.39	57.37	0.27	7.34	1.57	11.53	99.46
Stdev	0.23	0.67	0.24	0.39	0.10	0.17	0.69
Apfu	4.00	1.66	0.03	0.41	0.14	0.95	

This is the peer-reviewed, final accepted version for American Mineralogist, published by the Mineralogical Society of America.
The published version is subject to change. Cite as Authors (Year) Title. American Mineralogist, in press.
DOI: https://doi.org/10.2138/am-2023-9000. http://www.minsocam.org/

TABLE 3. Powder X-ray diffraction data for ruizhongite

I_{cal}(%)	I_{obs}(%)	d_{calc}(Å)	d_{obs}(Å)	*h k l*	I_{cal}(%)	d_{calc}(Å)	*h k l*
16.6		5.738		1 1 2	7.0	1.592	2 5 7
6.1		4.970		0 2 2	23.9	1.571	0 4 8
5.7		4.445		0 1 3	5.3	1.516	1 6 7
100.0	**100**	**3.757**	**3.755**	**1 2 3**	**7.3**	**1.450**	**3 6 7**
88.1	**76**	**3.514**	**3.511**	**0 0 4**	**10.0**	**1.435**	**4 4 8**
9.1		3.143		0 2 4	3.5	1.392	2 7 7
80.2	**73**	**2.997**	**2.992**	**2 3 3**	**2.5**	**1.378**	**0 2 10**
8.3		2.869		2 2 4	2.9	1.340	5 6 7
10.1		2.757		1 3 4	2.9	1.294	3 3 10
12.5	**21**	**2.566**	**2.574**	**1 2 5**	**1.7**	**1.283**	**2 4 10**
84.1	**79**	**2.485**	**2.482**	**0 4 4**	**1.7**	**1.252**	**1 5 10**
25.6	**46**	**2.280**	**2.276**	**2 3 5**	**4.7**	**1.242**	**0 8 8**
13.0	12	2.222	2.220	0 2 6	2.5	1.214	3 5 10
5.1		2.169		1 4 5			
19.7	**24**	**2.072**	**2.075**	**1 3 6**			
12.4	18	2.029	2.027	4 4 4			
14.9		1.913		3 3 6			
24.4	**39**	**1.785**	**1.784**	**2 3 7**			
11.9	19	1.757	1.753	0 0 8			
11.7	25	1.680	1.680	3 5 6			
3.3		1.657		2 2 8			

Note: The strongest lines are given in bold.

This is the peer-reviewed, final accepted version for American Mineralogist, published by the Mineralogical Society of America.
The published version is subject to change. Cite as Authors (Year) Title. American Mineralogist, in press.
DOI: https://doi.org/10.2138/am-2023-9000. http://www.minsocam.org/

TABLE 4. Information on structural refinement for ruizhongite

Crystal data	
Structural formula	$(Ag_{0.42}Pb_{0.18}Zn_{0.15}Fe_{0.03})Pb_{1.5}Ge_1S_4$
Formula weight	606.14
Crystal size/mm^3	0.006*0.005*0.004
Crystal system	cubic
Space group	$I\bar{4}3d$ (#220)
Unit cell dimensions	a = 14.0559(2) Å
Volume	2777.00(12) Å^3
Z	8
Density (calculated)	5.799 g/cm^3
Data collection and refinement	
Instrument	Rigaku Synergy
Radiation, wavelength, temperature	Cu $K\alpha$, 1.54184 Å, 293(2) K
F(000)	4143.0
2θ range (°)	15.442 to 152.764
Total reflections	2594
Unique ref (all)	471
Unique ref [$I > 4\sigma(I)$]	447
R_{int}	0.0419
R_σ	0.0296
Range of h, k, l	$-12 \le h \le 17$; $-17 \le k \le 13$; $-16 \le l \le 17$
R_1, wR_2 [$I > 4\sigma(I)$]	R_1 = 0.0298, wR_2 = 0.0666
R_1, wR_2 [all data]	R_1 = 0.0323, wR_2 = 0.0676
Goodness-of-fit	1.088
No. of parameters, restraints	26, 0
Maximum and minimum residual peak (e Å^{-3})	1.00/-1.15
Flack parameter	-0.034(17)

This is the peer-reviewed, final accepted version for American Mineralogist, published by the Mineralogical Society of America.
The published version is subject to change. Cite as Authors (Year) Title. American Mineralogist, in press.
DOI: https://doi.org/10.2138/am-2023-9000. http://www.minsocam.org/

TABLE 5. Atomic coordinates, isotropic displacement parameters (in Å^2) and bond valence sum for ruizhongite

Site	*Wyck.*	s.o.f.	*x/a*	*y/b*	*z/c*	U_{eq}	BVS
Ag1	24*d*	$Ag_{0.28}Pb_{0.12}Zn_{0.10}Fe_{0.02}$	0.40047(27)	0	1/4	0.0423(14)	0.46
Pb1	24*d*	$Pb_{1.00}$	1/4	0.00818(8)	0	0.0325(3)	1.71
Ge1	16*c*	$Ge_{1.00}$	0.22321 (12)	0.22321 (12)	0.22321 (12)	0.0158(6)	3.99
S1	16*c*	$S_{1.00}$	0.06534(25)	0.06534(25)	0.06534(25)	0.0126(12)	2.16
S2	48*e*	$S_{1.00}$	0.32215(37)	0.14666(38)	0.12811 (34)	0.0335(11)	1.68

Note: Bond valence sums (BVS) are calculated using the parameters of Brese and O'Keeffe (1991).

This is the peer-reviewed, final accepted version for American Mineralogist, published by the Mineralogical Society of America.
The published version is subject to change. Cite as Authors (Year) Title. American Mineralogist, in press.
DOI: https://doi.org/10.2138/am-2023-9000. http://www.minsocam.org/

TABLE 6. Selected bond distances and angles of ruizhongite

For GeS_4 tetrahedra		For PbS_4 pyramid	
Ge1—S1$^{\times1}$	2.242(5) Å	Pb1—S1$^{\times2}$	2.868(5) Å
—S2$^{\times3}$	2.208(6) Å	—S2$^{\times2}$	2.839(6) Å
Mean	2.217 Å	Mean	2.854 Å
S1—S2$^{\times3}$	3.543(8) Å	<S1—Pb1—S2>	71.81(13)°, 85.88(13)°
S2—S2$^{\times3}$	3.687(9) Å	For AgS_4 quadrangle	
<S1—Ge1—S2>	105.50(18)°	Ag1—Ag1	0.717(9) Å
<S2—Ge1—S2>	113.13(13)°	Ag1—S2	2.898(6), 2.708(6) Å
		<S2—Ag1—S2>	93.10(6)°

This is the peer-reviewed, final accepted version for American Mineralogist, published by the Mineralogical Society of America.
The published version is subject to change. Cite as Authors (Year) Title. American Mineralogist, in press.
DOI: https://doi.org/10.2138/am-2023-9000. http://www.minsocam.org/

TABLE 7. Comparative characteristics of ruizhongite with synthetic $(AgPb_{0.5})Pb_3Ge_2S_8$, $PbPb_3Ge_2S_8$, $(CuPb_{0.5})Pb_3Ge_2S_8$

Name	Ruizhongite*	Synthetic†	Synthetic‡	Synthetic†
Empirical formula	$(Ag_{0.82}Pb_{0.32}Zn_{0.28}Fe_{0.06})$ $Pb_3Ge_2S_8$	$(AgPb_{0.5})Pb_3Ge_2S_8$	$PbPb_3Ge_2S_8$	$(CuPb_{0.5})Pb_3Ge_2S_8$
Space group	$I\bar{4}3d$	$I\bar{4}3d$	$I\bar{4}3d$	$I\bar{4}3d$
a(Å)	14.0559	14.0291	14.096	13.8145
V(Å^3)	2777.00	2761.15	2800.84	2636.36
Ge-S distance(Å)	2.217	2.217	2.220	2.214
M-S distance(Å)	2.854	2.845	2.865	3.052
A-S distance(Å)	2.803	2.759	2.998	2.371
<S1—Ge—S2>	105.5	105.1	106.05	107.87
<S2—Ge—S2>	113.13	113.47	112.67	111.03
<S1—M—S2>	71.81°, 85.88(13)°	71.95°, 86.18°	71.41°, 85.25°	70.56°, 88.83°
<S2—A—S2>	93.10(6)°	92.06°	92.13°	95.6°

Notes: * this study; † Iyer *et al.* (2004); ‡Poduska *et al.* (2002).

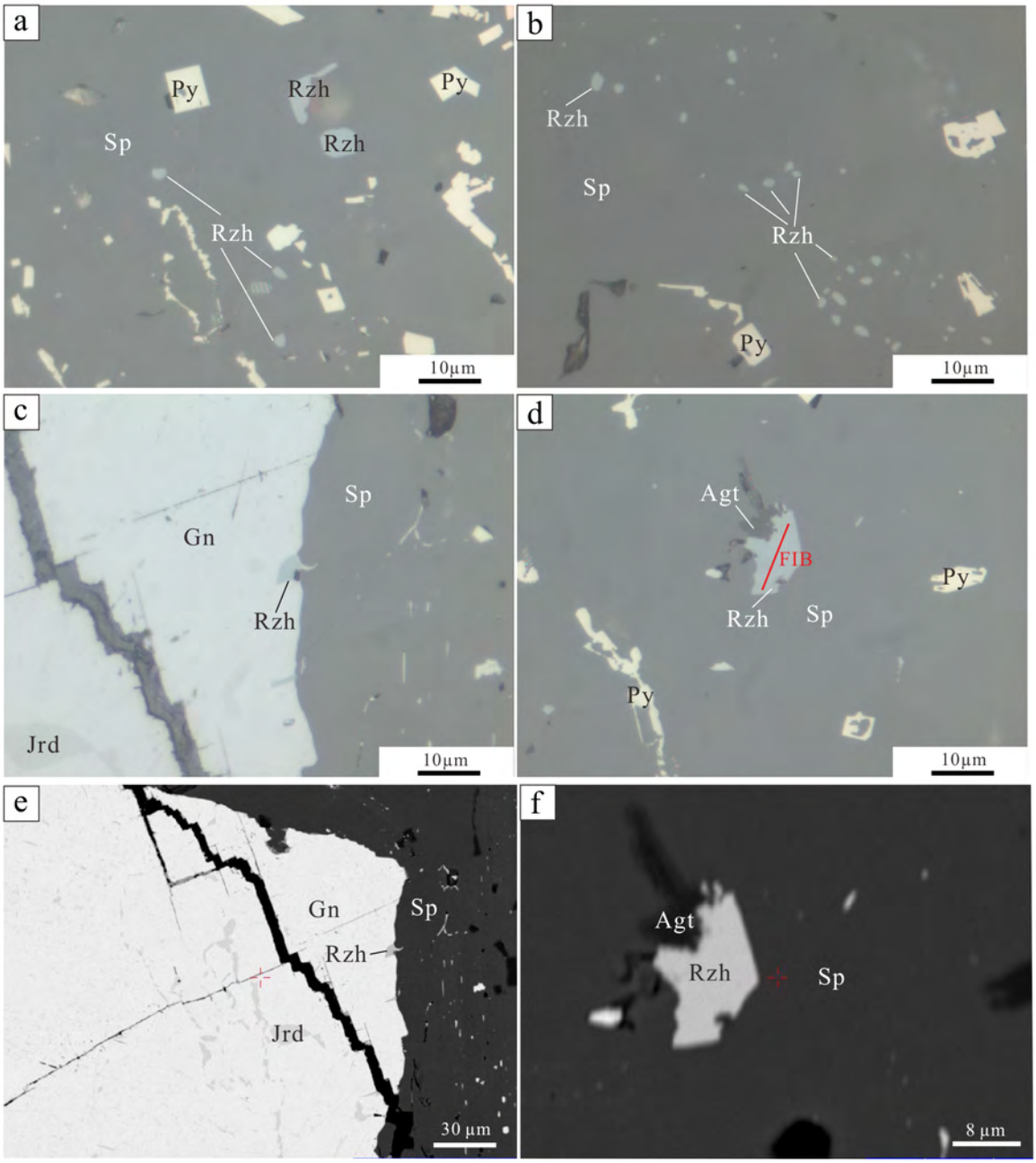

Fig. 1

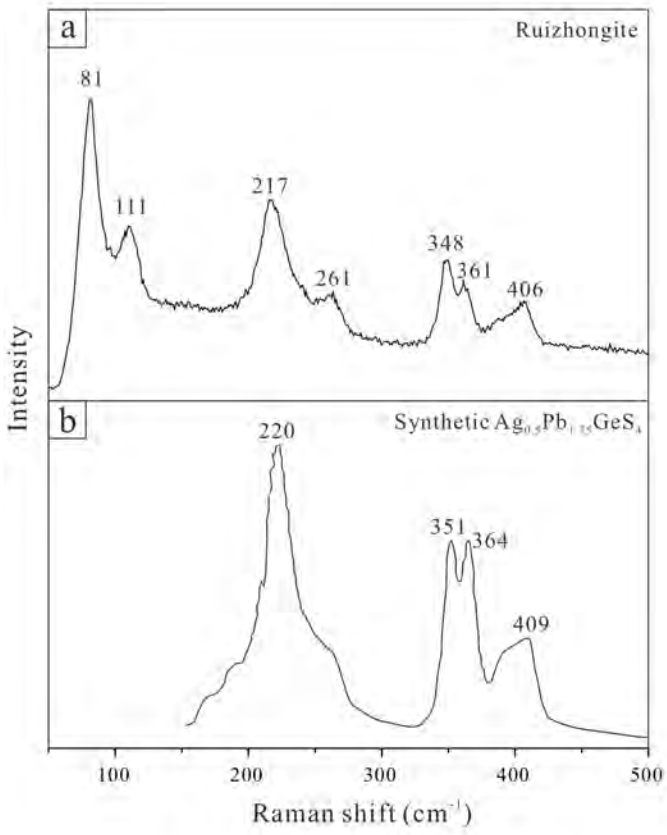

Fig. 2

This is the peer-reviewed, final accepted version for American Mineralogist, published by the Mineralogical Society of America.
The published version is subject to change. Cite as Authors (Year) Title. American Mineralogist, in press.
DOI: https://doi.org/10.2138/am-2023-9000. http://www.minsocam.org/

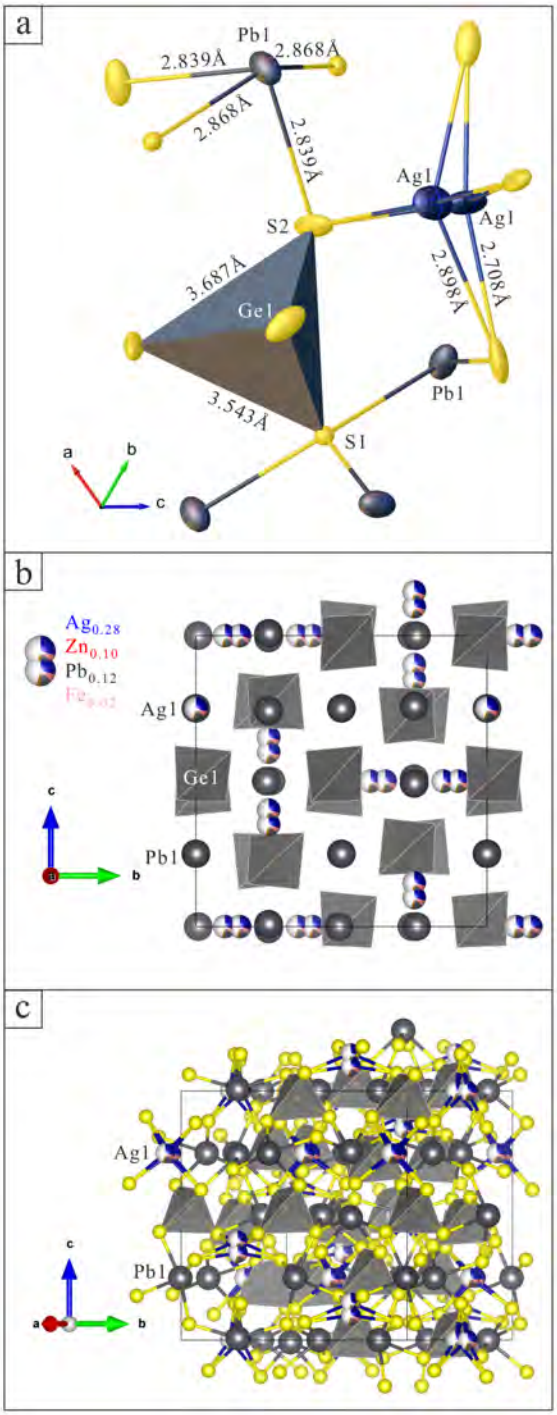

Fig. 3